Properties of the Vacuum.
2. Electrodynamic*

JAN AMBJØRN[†] AND STEPHEN WOLFRAM[‡]

California Institute of Technology, Pasadena, California 91125

The behaviour of a charged scalar field in an external electric field is discussed. Vacuum polarization is calculated by explicit summation of modes. Instabilities encountered in the external field approximation are absent when back reaction effects are included through a self-consistent semiclassical procedure.

1. INTRODUCTION

This is the second in a series of papers on the "bulk" properties of quantized fields. The first paper in the series [1] derived mechanical and thermodynamic properties of non-interacting quantized fields in finite volumes. The present paper discusses electrodynamic properties of quantized fields by considering the response of the "vacuum" state to external electric fields. The third paper in the series will discuss the response of quantized fields to external gravitational fields [2].

For simplicity, we consider primarily charged scalar fields in $1 + 1$ spacetime dimensions. The fields are confined to a finite spatial interval, so that their modes are discrete, and may be found explicitly.

In Section 2, we give a formal description of the modes and vacuum state for a charged scalar field φ in an external electric field. Section 3 treats in some detail the simple case of a φ field satisfying Dirichlet boundary conditions. For weak external electric fields, the ground state of the φ field exhibits vacuum polarization and behaves like a polarizable macroscopic medium, partially screening the applied electric field. Section 3 also considers nonclassical phenomena and instabilities which appear for larger electric fields.

Section 4 treats φ fields with general boundary conditions. In some cases, "vacuum polarization" is found to "antiscreen" the applied electric field, rather than screening like a polarizable medium. This behaviour is connected with the appearance of instabilities.

Sections 3 and 4 use the "external field approximation," which accounts for the

33

effect of the external electric field on the modes of the φ field, but ignores the electromagnetic "back reaction" of the φ field on itself. Section 5 describes a self-consistent semiclassical procedure which includes the effects of the back reaction. This procedure yields accurate results for large external electric fields so long as the charge on the φ field is sufficiently small. Instabilities which appeared in the external field approximation are found to be absent when back reaction effects are included.

2. PRELIMINARIES

This section considers the formal description of a charged spin zero (scalar) field in a static external electric field.[1] The following sections use this formalism to discuss the detailed behaviour of the "vacuum" in the presence of an electric field.

The Klein–Gordon Lagrangian for a complex scalar field φ with mass m and charge e minimally coupled to an electromagnetic field A_μ is

$$\mathbf{L} = |D_\mu \varphi|^2 - m^2 |\varphi|^2 - \tfrac{1}{4} F_{\mu\nu}^2 - j_\mu^{\text{ext}} A_\mu, \tag{2.1}$$

$$D_\mu \equiv \partial_\mu + ieA_\mu,$$

$$F_{\mu\nu} \equiv \partial_\mu A_\nu - \partial_\nu A_\mu,$$

where j_μ^{ext} is an external electromagnetic current. This yields the equations of motion

$$(D_\mu^2 + m^2) = 0, \tag{2.2a}$$

$$\partial^\mu F_{\mu\nu} = j_\nu^\varphi + j_\nu^{\text{ext}}, \tag{2.2b}$$

where

$$j_\nu^\varphi = ie[\varphi^* D_\nu \varphi - (D_\nu \varphi)^* \varphi] \tag{2.2c}$$

is the conserved electric current for the φ field. The φ charge density ρ is defined as $\rho = j_0^\varphi$. Choosing Coulomb gauge $\partial_i A_i = 0$. Eq. (2.1) yields the Hamiltonian density for the φ field

$$\mathbf{H} = |\pi|^2 + |D_i \varphi|^2 + m^2 |\varphi|^2 - A_i j_i^{\text{ext}} + \tfrac{1}{2} E_L^2 + \tfrac{1}{2}(E_T^2 + B^2), \tag{2.3a}$$

where π is the canonical momentum

$$\pi = (D_0 \varphi)^*. \tag{2.3b}$$

With Coulomb gauge, the longitudinal (Coulomb) electric field E_L in the penultimate term of Eq. (2.3) is constrained by

$$\nabla \cdot E_L = -\nabla^2 A_0 = \rho + \rho^{\text{ext}}. \tag{2.4}$$

[1] For reviews, see [3–5].

In the last term of Eq. (2.3), E_T and B are the transverse electric field and the magnetic field, and represent dynamical degrees of freedom in the electromagnetic field. (A total divergence term $\nabla \cdot (A_0 E_L)$ does not contribute in the charge zero sector, and is dropped in Eq. (2.3) and below.) Introducing the electric displacement D and polarization P according to

$$\nabla \cdot P = -\rho,$$

$$\nabla \cdot D = \rho^{\text{ext}}, \tag{2.5}$$

the Hamiltonian density (2.3a) becomes

$$\mathbf{H} = (|\pi|^2 + |D_i\varphi|^2 + m^2 |\varphi|^2 + \rho A_0) + \tfrac{1}{2}(D^2 - P^2) - A_i j_i^{\text{ext}}$$
$$+ \tfrac{1}{2}(E_T^2 + B^2). \tag{2.6}$$

Sections 3 and 4 and the remainder of this section consider the external field approximation. This approximation consists in taking a quantized φ field with a fixed classical external electric field, and ignoring the back reaction of the charged φ field on the electric field and transverse photon contributions. The effective Hamiltonian in this case is obtained from Eq. (2.6) by setting E_T, B and j_i^{ext} to zero, and using the relation between A_0 and ρ^{ext} in Coulomb gauge

$$\mathbf{H}^\varphi = |\pi|^2 + |D_i\varphi|^2 + m^2 |\varphi|^2 + \rho A_0$$
$$-\nabla^2 A_0 = \nabla \cdot E = \rho^{\text{ext}}. \tag{2.7}$$

The total charge of the φ field (in d space dimensions)

$$Q = \int d^d x \, \rho(x) = ie \int d^d x \, (\varphi^* \pi^* - \varphi\pi) \tag{2.8}$$

for solutions to Eq. (2.2a) is conserved if φ satisfies appropriate gauge invariant boundary conditions. In the systems considered below, the electric charge is usually confined to a finite volume with boundary σ, so that

$$\int_\sigma dn_i \cdot j_i^{\text{ext}} = 0, \tag{2.9}$$

where n_i is the outward normal to σ. The field φ must thus satisfy a boundary condition of the form

$$n_i D^i \varphi + \chi(\sigma) \, \varphi = 0, \tag{2.10}$$

where χ is a real function.

The boundary condition (2.10) may be implemented in the Lagrangian (2.1) by the introduction of a source term

$$\delta\mathbf{L} = -\chi(\sigma(x)) \, \delta(x - \sigma) |\varphi|^2 \tag{2.11}$$

We take a classical static external electric field E_i. A gauge may be chosen in this case so that A_0 is time independent, and determined up to a constant by

$$E_i = -\partial_i A_0(x). \tag{2.12}$$

The linearity of (2.2a) then allows its solutions to decomposed into normal modes of definite frequency:

$$\varphi_n(x, t) = \varphi_n(x)\, e^{-i\Omega_n t}, \tag{2.13a}$$

$$(\Omega_n - eA_0)^2 \, \varphi_n(x) = (-\nabla^2 + m^2)\, \varphi_n(x). \tag{2.13b}$$

The addition of a constant V to A_0 corresponds to a gauge transformation with parameter $-Vt$, leading to a phase change e^{-ieVt} in φ_n and hence a displacement of Ω_n:

$$\Omega_n \to \Omega_n + eV. \tag{2.14}$$

The hermiticity of the operator ∇^2 with the boundary condition (2.10) (and $A_i = 0$) implies the relation

$$(\Omega_n - \Omega_m{}^*) \int d^d x [\Omega_n + \Omega_m{}^* - 2eA_0(x)]\, \varphi_m{}^*(x)\, \varphi_n(x) = 0. \tag{2.15}$$

For real $\Omega_{n,m}$, this yields

$$\int d^d x (\Omega_n + \Omega_m - 2eA_0(x))\, \varphi_m{}^*(x)\, \varphi_n(x) = 0 \qquad (\Omega_m \neq \Omega_n). \tag{2.16}$$

For complex Ω_n,

$$\int d^d x [\mathrm{Re}\, \Omega_n - eA_0(x)]\, |\varphi_n(x)|^2 = 0. \tag{2.17}$$

In classifying solutions, it is convenient to rewrite Eq. (2.2) as an ordinary first-order (Schrodinger-like) eigenvalue equation:

$$i\frac{\partial}{\partial t}\, \Psi = H\Psi, \tag{2.18a}$$

$$\partial^\mu F_{\mu\nu} = -e\Psi^* \sigma_2\, \Psi, \tag{2.18b}$$

$$H\Psi_n = \Omega_n \Psi_n, \tag{2.18c}$$

$$\Psi = \begin{pmatrix} \varphi \\ \pi^* \end{pmatrix}, \tag{2.18d}$$

$$H = \begin{pmatrix} eA_0 & 0 \\ 0 & eA_0 \end{pmatrix} + i \begin{pmatrix} 0 & 1 \\ -D_i^2 + m^2 & 0 \end{pmatrix}, \tag{2.18e}$$

$$\sigma_2 = \begin{pmatrix} 0 & -i \\ i & 0 \end{pmatrix}. \tag{2.18f}$$

With the boundary conditions (2.10), H is an hermitean operator with respect to the indefinite scalar product

$$\langle \Psi_1 | \Psi_2 \rangle = -\int d^d x\, \Psi_1 {}^* \sigma_2 \Psi_2 = i \int d^d x\, (\varphi_1 {}^* \pi_2 {}^* - \pi_1 \varphi_2). \qquad (2.19)$$

Comparison with Eq. (2.8) reveals that the norm $\langle \Psi | \Psi \rangle$ gives the total charge (in units of e) for the Ψ state. Similarly, Eq. (2.3) shows that $\langle \Psi | H | \Psi \rangle = \int d^d x\, \mathbf{H}(\varphi)$.

Equation (2.16) expresses the orthogonality of the eigenfunctions Ψ_m, Ψ_n with respect to the scalar product (2.19) for real eigenvalues Ω_m, Ω_n.

For some A_0, eigenfunctions with complex eigenvalues Ω_n exist [3, 4, 6]. The φ fields associated with these eigenfunctions exhibit a real exponential time dependence. Equation (2.17) implies that all eigenfunctions with complex eigenvalues have zero norm. If Ψ_n is an eigenfunction with eigenvalue Ω_n, $\Psi_n {}^*$ is an eigenfunction with conjugate eigenvalue $\Omega_n {}^*$. The scalar product $\langle \Psi_n | \Psi_n {}^* \rangle$ is almost always non-zero. It vanishes only for exceptional A_0, at which an additional class of solutions to Eq. (2.18) with $te^{i\Omega t}$ time dependence exist. These solutions correspond to the "associated eigenfunctions" $\tilde{\Psi}$ satisfying the equation [7]

$$H\tilde{\Psi}_n = \Omega_n \tilde{\Psi}_n + \Psi_n. \qquad (2.20)$$

The first step in the second quantization of the φ field is to determine the normalization of the eigenfunctions φ_n. The eigenfunctions with real eigenvalues may be normalized to have total charge $\pm e$. (Note that while the magnitude of the charge associated with φ_n can be modified by normalization, its sign cannot.) Normal modes with positive charge are interpreted as "particle" solutions, and those with negative charge as "antiparticle" solutions. The energy of a "particle" solution is given by its corresponding eigenvalue Ω_n, while for an "antipaticle" solution, the energy is $-\Omega_n$.

At the exceptional points for which the charge deduced from the scalar product (2.19) vanishes, the modes may be normalized so that $\langle \tilde{\Psi}_n | \Psi_n \rangle = 1$. For complex eigenvalues, a possible normalization is $\langle \Psi_n | \Psi_n {}^* \rangle = i$.

We shall assume that the eigenfunctions Ψ_n (including, when necessary, "associated" and complex eigenfunctions) form a complete set of functions with the boundary conditions (2.10). A proof of this result is outlined in Ref. [7].

The second quantization of the φ field is simplest when A_0 is such that all eigenvalues are real, and positive and negative norm eigenfunctions have eigenvalues $\Omega_m^{(+)}$ and $\Omega_n^{(-)}$, respectively, such that $\Omega_m^{(+)} > \Omega_n^{(-)}$ for all n, m. This case is often realized in weak electric fields, as discussed in Section 3. Decomposing φ in terms of positive and negative norm eigenfunctions

$$\varphi(x, t) = \sum_{\Omega_m^{(+)}} a_m \varphi_m^{(+)}(x)\, e^{-i\Omega_m^{(+)} t} + \sum_{\Omega_n^{(-)}} b_n^+ \varphi_n^{(-)}(x)\, e^{-i\Omega_n^{(-)} t} \qquad (2.21)$$

the equal-time canonical commutation relations

$$[\varphi(x, t), \pi(y, t)] = i\delta(x - y) \qquad (2.22)$$

imply

$$[a_m, a_n^+] = \delta_{nm}, \qquad (2.23)$$
$$[b_m, b_n^+] = \delta_{nm}$$

for the operator-valued expansion coefficients a_n, b_n.

The vacuum state $|0_E\rangle$ in the presence of the external electric field is defined such that

$$a_n |0_E\rangle = b_n |0_E\rangle = 0. \qquad (2.24)$$

The "induced charge density" in this state is given by

$$\rho^I(x) = \langle 0_E | \hat{\rho}(x) | 0_E \rangle,$$
$$\hat{\rho} = \frac{ie}{2} [\varphi^+ \pi^+ + \pi^+ \varphi^+ - \varphi\pi - \pi\varphi]. \qquad (2.25)$$

Hence

$$\rho^I(x) = \tfrac{1}{2} \sum_n (\rho_n^{(+)}(x) + \rho_n^{(-)}(x)), \qquad (2.26)$$

where $\rho_n^{(\pm)}$ are the charge densities associated with the modes $\varphi_n^{(\pm)}$. As expected, each possible mode of the field contributes with weight $\frac{1}{2}$ in the vacuum state.

The "vacuum polarization" is given in terms of the induced charge density (2.25) in analogy with the classical equation (2.5) by

$$\nabla \cdot P(x) = -\rho^I(x),$$
$$D(x) = E(x) + P(x) = \varepsilon(x)\, E(x), \qquad (2.27a)$$

where ε is the "dielectric constant of the vacuum." The electric field is taken here to be classical, as assumed below. Since the net charge of the φ field is conserved, the electric displacement satisfies

$$\nabla \cdot D(x) = \rho^{\text{ext}}. \qquad (2.27b)$$

The presence of the external electric field causes a shift in the φ energy eigenvalues, and hence in the vacuum energy, given by

$$H^\varphi(E) - H^\varphi(0) = \tfrac{1}{2} \sum_n [(\Omega_n^{(+)} - \Omega_n^{(-)}) - (\Omega_n^{(0)(+)} - \Omega_n^{(0)(-)})] \qquad (2.28)$$

where the $\Omega^{(0)}$ are the energy eigenvalues for zero external electric field. Note that while $\Omega_n^{(+)}$ and $\Omega_n^{(-)}$ both change under a gauge transformation, their difference is gauge invariant. An induced φ charge density modifies the classical electric field, as in Eq. (2.27). The energy (2.28) may be considered as the effective potential for the electric field calculated to the one loop approximation in the φ field.

Even when positive and negative charge eigenvalues do not form separated sequences, the expansion (2.21) remains formally correct so long as all eigenvalues are real and non-zero. However, as discussed below, the energy in such a case is not bounded below, and no ground state may therefore be identified [3].

When complex eigenvalues $\Omega_n^{(c)}$ exist, straightforward second quantization of the scalar field is no longer possible. An expansion of the form (2.21) may still be used if terms corresponding to the complex modes are added [7]:

$$\sum_{\Omega^{(c)}} (c_n \varphi_n^{(c)} e^{-i\Omega_n^{(c)}t} + d_n \varphi_n^{(c)}* e^{-i\Omega_n^{(c)}*t}), \tag{2.29a}$$

$$[d, c^+] = -[c, d^+] = i, \tag{2.29b}$$

$$[d, d^+] = [c, c^+] = [c, d] = 0. \tag{2.29c}$$

The charge of the φ field remains quantized in this case, but the energy is no longer discrete. The energy operator for the complex modes is $H_n = \mathrm{Re}\,\Omega_n^{(c)} + i(\Omega_n d^+ c - \Omega_n^* c^+ d)$, and has a continuous spectrum covering all real eigenvalues. Again, no ground state may be defined.

3. External Field Approximation: Dirichlet Boundary Conditions

This section uses the formalism introduced in Section 2 to discuss in some detail the behavior of a massless charged scalar field φ in $1+1$ spacetime dimensions subject to a static external electric field E. The field is restricted to the finite region $0 < Z < a$, and satisfies the boundary conditions (2.9), (2.10) with $\chi = \infty$, so that $\varphi(0) = \varphi(a) = 0$ (Dirichlet boundary conditions). It is convenient to introduce the dimensionless variables

$$z = Z/a,$$
$$\lambda = eEa^2,$$
$$\varepsilon = ea,$$
$$\omega = a\Omega_{(\alpha)} + \lambda\alpha, \tag{3.1}$$

where α is a gauge parameter, and ω is gauge invariant. Notice that in $1+1$ dimensions, the electric charge e has dimensions of mass. The field satisfies the Klein–Gordon equation (2.2a) with $A_0 = -\lambda[(z - \tfrac{1}{2}) + \alpha]$

$$\left(\left[\omega_n + \lambda\left(z - \frac{1}{2}\right)\right]^2 + \frac{d^2}{dz^2}\right)\varphi_n(z) = 0, \tag{3.2a}$$

$$\varphi_n(0) = \varphi_n(1) = 0. \tag{3.2b}$$

The charge density associated with the field is obtained from (2.5c) and is given by

$$\rho_n(z) = \varepsilon(\omega_n + \lambda(z - \tfrac{1}{2})) |\varphi_n(z)|^2. \tag{3.3}$$

Here, as below, ρ denotes a dimensionless charge density obtained by multiplication of the complete charge density by a^2. For gauge dependent results, we choose $\alpha = \tfrac{1}{2}$. With this symmetrical choice, each positive eigenvalue ω_n has an associated negative eigenvalue $-\omega_n$. The charge densities of the corresponding modes are related by $\rho_n^+(z) = -\rho_n^-(1-z)$ (so long as symmetrical boundary conditions are used).

When no electric field is applied ($\lambda = 0$), the modes of the φ field are given by $\varphi_n(z) = \sin(n\pi z)$ with $\omega_n = n\pi$, where n is an integer. The charge density of each mode is symmetrical about the point $z = \tfrac{1}{2}$.

For non-zero electric field ($\lambda \neq 0$), the modes are formally given by

$$\varphi_n(z) = a_1 D_{-1/2}((1+i)\sqrt{2}v) + a_2 D_{-1/2}(-(1-i)\sqrt{2}v)$$

$$= \frac{b_1}{\sqrt{v}} W_{0,-1/4}(iv^2) + \frac{b_2}{\sqrt{v}} W_{0,-1/4}(-iv^2)$$

$$= c_1 \sqrt{v} J_{1/4}\left(\frac{v^2}{2}\right) + c_2 \sqrt{v} N_{1/4}\left(\frac{v^2}{2}\right),$$

$$v = \sqrt{\lambda}\left(\left(z - \frac{1}{2}\right) + \omega_n\right), \tag{3.4}$$

where D_v is a parabolic cylinder function (e.g., [8]), $W_{\mu,v}$ is a Whittaker function, and J_v and N_v are respectively regular Bessel functions and Neumann functions. The possible eigenvalues ω_n could in principle be found from (3.4) by solving the transcendental equation obtained from $\varphi(1) = \varphi(0) = 0$.

The form of the modes φ_n for small λ may be obtained from perturbation theory. To first order in λ,

$$\varphi_n(z) = \frac{1}{\sqrt{\pi n}}\left[\sin(n\pi z)\left(1 + \frac{\lambda}{2\pi n}\left(\frac{1}{2} - z\right)\right) - \cos(n\pi z)\frac{\lambda}{2}z(1-z)\right]. \tag{3.5}$$

The total charge density associated with the nth positive and negative mode in this approximation is given by

$$\rho_n^I(z) = \tfrac{1}{2}[\rho_n^{(+)}(z) + \rho_n^{(-)}(z)] = -\varepsilon\lambda z(1-z)\sin(2\pi n z). \tag{3.6}$$

In the absence of the external electric field ($\lambda = 0$) the charge densities of the positive and negative modes are equal and opposite for all values of z, and no net charge density exists: $\langle 0| \hat{\rho}(z) |0\rangle = 0$. Introduction of the electric field shifts the charge densities of the positive and negative modes oppositely ($\rho^{(-)}(z) = -\rho^{(+)}(1-z)$). The positively charged modes are shifted in the direction of the electric field, as expected

from classical considerations. The "centre of mass" for the charge density of the nth mode is given to first order in λ by

$$\langle z \rangle_n^{(\pm)} = \frac{1}{2} \pm \frac{3}{4} \frac{(-\lambda)}{(n\pi)^3}. \tag{3.7}$$

To this order, the total induced charge density is given by

$$\rho^I(z) = \sum_{n=1}^{\infty} \rho_n^I(z) = -\tfrac{1}{2}\varepsilon\lambda z(1-z)\cot(\pi z). \tag{3.8}$$

This charge density leads, as expected, to screening of the applied external electric field.

Figure 3.1a shows the exact form of the lowest positive energy mode for $\lambda = 5$ (full curve) and $\lambda = 0$ (dashed curve). The direction of the electric field corresponds to a positive charge on the left-hand boundary and a negative charge on the right-hand boundary. The positively charged mode shown is thus shifted to the right in the presence of the electric field.

Figure 3.1b gives the total charge density $\rho_1^I(z)$ associated with the lowest-energy positive and negative charge modes. The full curve is the exact result; the dashed curve is the first-order form (3.6). The $O(\lambda)$ approximation remains comparatively accurate even at $\lambda = 5$.

Figure 3.1c shows the distortion in the charge density of the $n = 2$ positive charge mode in the presence of an external electric field.

The total induced charge density is in principle obtained by summing the contributions from each mode, according to Eq. (2.26). However, as suggested by the
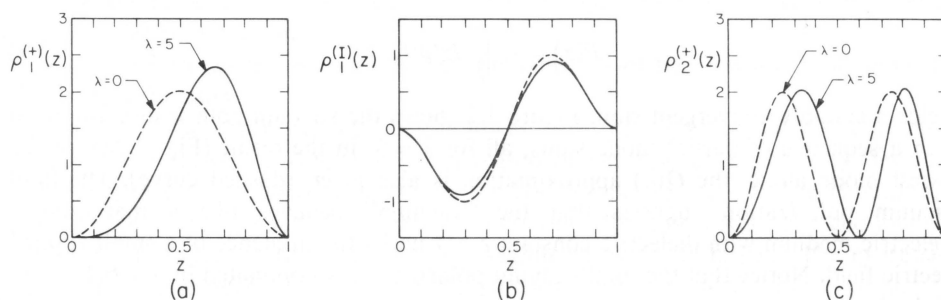

FIG. 3.1. Modifications in low modes of a unit charge massless scalar field φ in an external electric field of strength λ directed from left to right. The φ field is taken to vanish at $z = 0$ and $z = 1$ (Dirichlet boundary conditions). A symmetrical gauge is chosen. (a) Charge density for the lowest energy positively charged mode. (b) Total charge density for the lowest energy positive and negatively charged modes with $\lambda = 5$. Dashed line gives an approximate result obtained to first order in λ. (c) Charge density for the second positively charged mode.
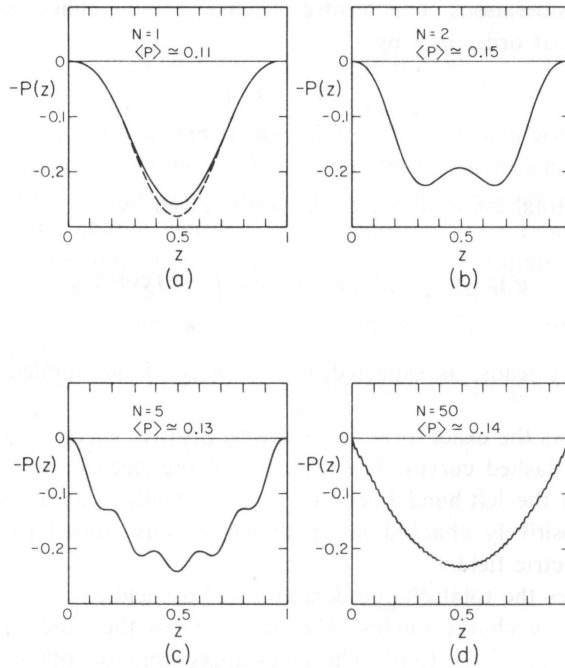
FIG. 3.2. Vacuum polarization for massless unit charge scalar field satisfying Dirichlet boundary conditions in a weak external electric field with strength $\lambda = 5$. The contributions from N positive and negative charge modes are included. In the case $N = 1$, the result obtained at first order in λ is shown (dashed curve).

perturbative result (3.6), the numerical convergence of the resulting sum is not adequate. Nevertheless, consideration of the induced electric field

$$P(z) = -\int_0^z dz' \rho^I(z') \tag{3.9}$$

yields a suitably convergent sum. Figure 3.2 shows the vacuum polarization obtained with a sequence of partial mode sums, all for $\lambda = 5$. In the result (Fig. 3.2a) for the lowest mode alone, the $O(\lambda)$ approximation is also given (dashed curve). The final vacuum polarization suggests that the "vacuum" behaves like a macroscopic dielectric medium with dielectric constant $\varepsilon > 1$ under the influence of a small applied electric field. Notice that the total vacuum polarization is dominated by the behaviour of the lowest mode.

Figure 3.3 shows the average vacuum polarization as a function of λ. The results show that the $O(\lambda)$ perturbative estimate remains accurate until $\lambda \gtrsim 10$.

Equation (3.2) assumes an external electric field uniform throughout the region $0 < z < 1$. As an alternative, one may take the field to be uniform only in the region $\frac{1}{2} - w < z < \frac{1}{2} + w$, and to vanish elsewhere. In the limit $w \to 0$, this corresponds to a
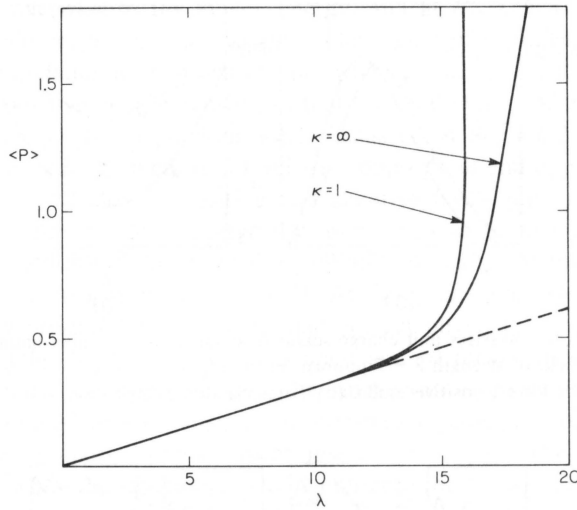
FIG. 3.3. Average vacuum polarization for massless unit charge scalar field satisfying Dirichlet boundary conditions, given as a function of the strength λ of the external electric field. κ labels the number of iterations in the self-consistent procedure used to account for back reaction effects. The dashed line gives the result obtained to first order in λ.

potential jump with an infinite associated electric field. Figure 3.4 shows results for $\lambda = 5$ and various w. The lowest mode is insensitive to short distance details of the electric field, and depends primarily on the total potential difference from $z = 0$ to $z = 1$.

The results above are for small external electric fields λ. We now discuss the case of large λ. Throughout this section, we use the external field approximation.[2] For large λ, the back reaction effects thus ignored become important. Their consequences are considered in Section 5.

Figure 3.5 shows the energies and charge densities of the first few positive energy levels as a function of λ.

For $\lambda \lesssim 8$, the charge density for the lowest positive energy, positive charge mode is positive everywhere. Above $\lambda \simeq 8$, a region of negative charge density develops. The integrated total charge nevertheless remains normalized to $+1$. The Hamiltonian (2.7) suggests that for large λ, it may be favourable for a positively charged mode to develop a negative charge density in the region where A_0 is largest. The expression (3.3) shows that negative charge density appears in the region $0 < z < \frac{1}{2} - \omega/\lambda$.

When $\lambda = 0$, the energy levels are equally spaced with $\omega_n = n\pi$. Only the kinetic energy term in (2.7) contributes for $\lambda = 0$. For small λ, the distortion of the charge density produces a small negative potential energy, which reduces the total energy of the mode. The effect is $O(\lambda^2)$ in a perturbation expansion. For large λ, the electric

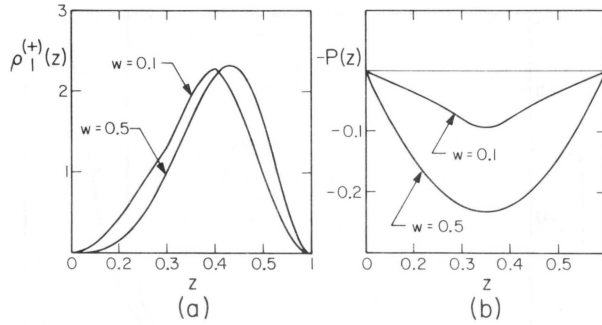[2] Some of the results here were also given in Ref. [3].

FIG. 3.4.   Results for massless unit charge scalar field satisfying Dirichlet boundary conditions with an external electric field of strength $\lambda = 5$ uniform in the region $\frac{1}{2} - w \ll z < \frac{1}{2} + w$ and zero elsewhere. (a) Charge density for lowest positive mode. (b) Total vacuum polarization.
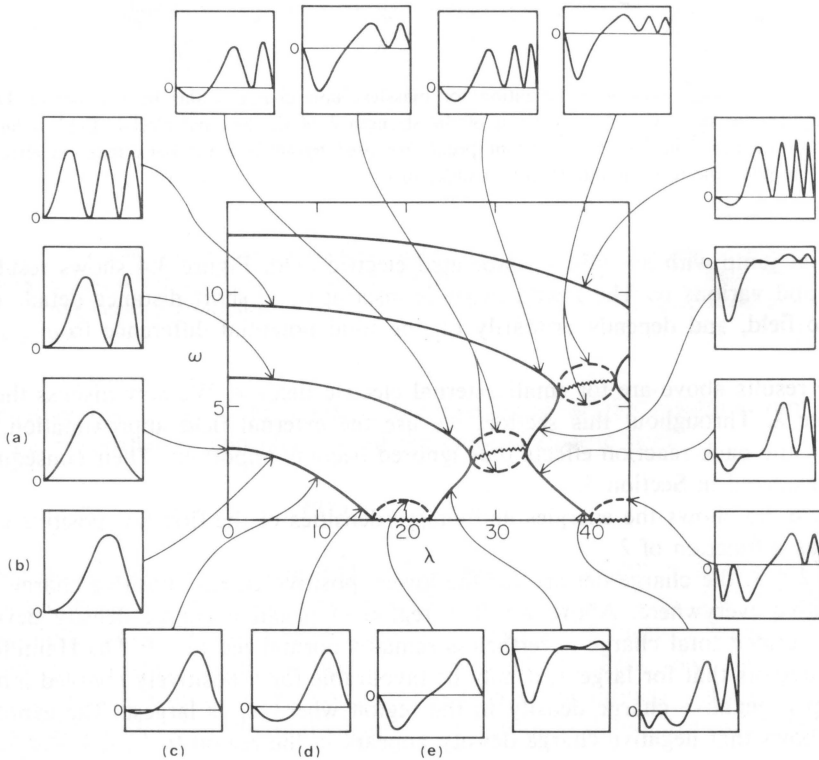

FIG. 3.5.   Energies and charge densities for first few positive energy levels of a massless charged scalar field satisfying Dirichlet boundary conditions in an external electric field of strength λ. For some values of λ, the eigenvalues ω are complex. In such regions, $\mathrm{Re}(\omega)$ is shown as a wavy curve. The vertical distance of the dashed curves indicates the value of $\mathrm{Im}(\omega)$. Cutting along the dashed lines and folding the upper half ellipses upwards and lower ones downwards yields a three-dimensional plot with the $\mathrm{Im}(\omega)$ axis out of the page.

potential energy overwhelms the kinetic energy, and at $\lambda = \lambda_c \simeq 16$, the total energy of the lowest mode drops vertically to zero. The region of negative charge density in the lowest mode expands as λ increases, and when λ reaches λ_c, it becomes as large as the region of positive charge density, so that the total charge of the mode vanishes. The formal aspects of this behaviour were discussed in Section 2. Each positive ω level in Fig. 3.5 is accompanied by a level with opposite ω and opposite total charge. Precisely at $\lambda = \lambda_c$, the lowest positive and negative levels join into a single mode with zero energy and zero total charge (but non-zero charge density). As mentioned in Section 2, an additional "associated eigenfunction" exists at this value of λ, and the ground state is no longer unique [3, 7]. At this point, the external field approximation therefore presumably ceases to yield correct physical results, even though it is formally possible to choose a vacuum state and perform canonical quantization [3, 7]. The self-consistent approach described in Section 5 avoids these difficulties.

Section 2 mentioned that in some cases, complex eigenvalues ω_n may occur. The first set of complex energy levels appear just above $\lambda = \lambda_c$. The real part of their energy vanishes, while the imaginary part is non-zero for $\lambda > \lambda_c$. The charge densities of the modes are shown in Fig. 3.5. As discussed in Sect. 2, the total charge obtained by integration of this charge density always vanishes.

Figure 3.5 shows that when $\lambda \gtrsim 23$, the pair of complex energy levels disappears, and a pair of positive and negative real energy levels appear. In the region $23 \lesssim \lambda \lesssim 27$, all eigenvalues are real. However, the lowest positive energy level has negative total charge and thus negative energy. The combination of this mode with its negative ω partner has zero charge and negative total energy -2ω. High occupation numbers in these modes lead to indefinitely negative energies and no definite vacuum state.

Figure 3.6a extends the energy levels shown in Figure 3.5 to higher values of λ. Curve segments with $\partial\omega/\partial\lambda < 0$ correspond to modes with positive charge and positive energy, and those with $\partial\omega/\partial\lambda > 0$ to negative modes [3, 4]. At each point of vertical tangency, a zero norm mode exists. Between each adjacent pair of vertical tangents extend a pair of complex ω modes. When these complex modes are included, each energy level in Figure 3.6a forms a continuous curve as a function of λ. The curve develops an imaginary part whenever it crosses another curve. The wave functions for all modes associated with a particular continuous curve exhibit the same number of nodes in the interval $0 < z < 1$. Notice that when $\lambda \to \infty$, the fraction of possible λ values at which no complex modes exist tends to zero.

The existence of real modes even at high λ is essential in obtaining known results [6] for the continuum limit of a uniform electric field throughout space. This limit corresponds to $a \to \infty$ and hence $\lambda \to \infty$. As $\lambda \to \infty$, the pattern of energy levels stabilizes, and the charge densities for real modes with $\omega \lesssim \lambda$ take on the form illustrated in Figure 3.7. The modes have positive charge density in the region $z > \frac{1}{2}$ and negative charge density in the region $z < \frac{1}{2}$. In the limit $a \to \infty$, the modes may be superposed to yield travelling waves carrying positive charge to the right and negative charge to the left, thereby corresponding to continuum modes, and allowing the interpretation of particle–antiparticle pair production.
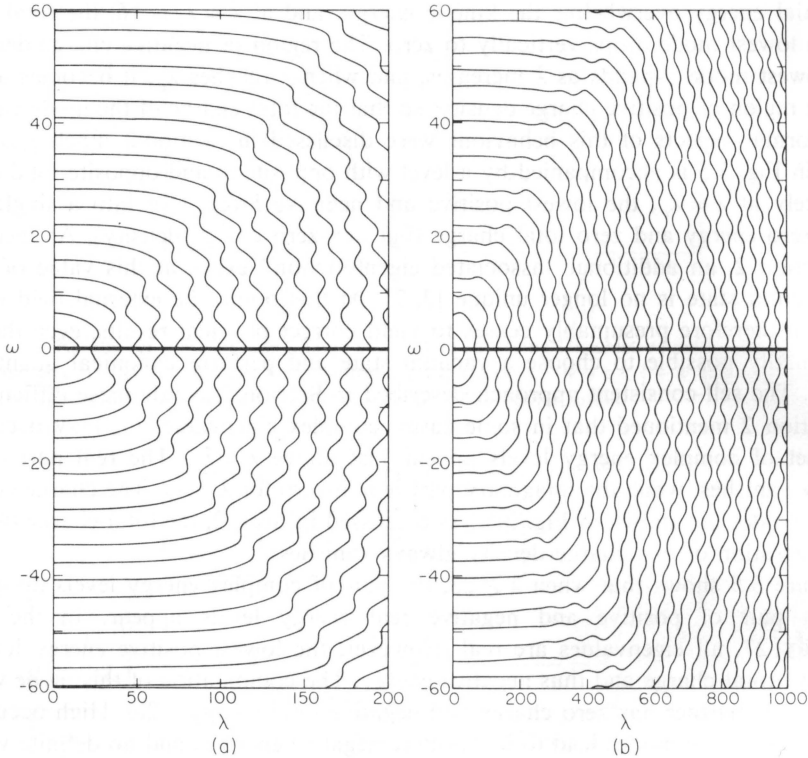
FIG. 3.6. Positive and negative energy levels for a massless charged scalar field satisfying Dirichlet boundary conditions with an applied external electric field of strength λ. (a) Electric field uniform throughout region $0 < z < 1$; (b) electric field uniform for $0.4 < z < 0.6$, and zero elsewhere. Between each pair of vertical tangent points, a pair of complex energy eigenvalues exist. Curve segments with $\partial\omega/\partial\lambda < 0$ have positive charge and positive energy; others have negative charge and negative energy.

In finite systems, each mode is normalized if possible to unit total charge. In an infinite system, modes are normalized to give particle wave functions with unit charge density. Complex energy modes exhibit real exponential growth modulated by an oscillating factor in both time and space (see Eq. (3.4)). The oscillating factor allows modes to satisfy the necessary boundary conditions. However, away from the boundaries, the real exponential factor give rise to exponentially large charge densities. The normalized modes thus have exponentially small charge densities except in an exponentially small region. In the limit $\lambda \to \infty$, the normalized complex energy modes have zero charge density almost everywhere, and are therfore of no physical relevance.

The energy levels shown in Figure 3.6a assume that a uniform electric field exists throughout the region $0 < z < 1$. Figure 3.6b shows the energy levels obtained with a field uniform between $z = 0.4$ and $z = 0.6$, and zero elsewhere. The results in Figs. 3.6a and 3.6b are qualitatively similar. The qualitative independence of the results on
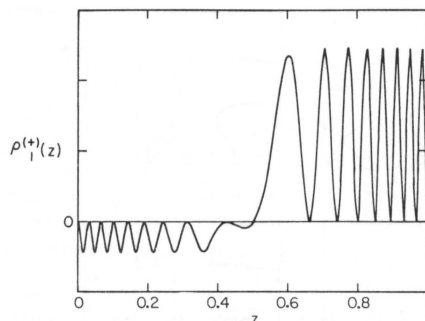
FIG. 3.7. Charge density for lowest positive energy level of scalar field with Dirichlet boundary conditions in an electric field of strength $\lambda = 200$. Separation into positive and negative "particle" regions is evident.

the width of the electric field reflect the similarity of particle production in a uniform electric field and a step potential.

4. EXTERNAL FIELD APPROXIMATION: GENERAL BOUNDARY CONDITIONS

According to Eq. (2.10) the most general charge-conserving boundary conditions for a massless scalar field in $1 + 1$ dimensions have the Robin form

$$\frac{\partial \varphi(0)}{\partial z} = h_0 \varphi(0),$$

$$\frac{\partial \varphi(0)}{\partial z} = -h_1 \varphi(1). \tag{4.1}$$

Section 3 considered the special case $h_0 = h_1 = \infty$, corresponding to Dirichlet boundary conditions.

We discuss first the implementation of the boundary conditions (4.1) in the absence of an external electric field ($\lambda = 0$). In this case, Eq. (2.2) is the equation of motion for a classical vibrating string with amplitude $\varphi(z, t)$. The boundary conditions (4.1) specify the string to be attached at its two ends by elastic forces $F_\alpha = -h_\alpha \varphi(\alpha, t)$ ($\alpha = 0, 1$). Equations (2.2) and (4.1) form a standard Sturm–Liouville system in this case. If one of the h_α is negative, larger negative potential energy is achieved by increasing $\varphi(\alpha, t)$, and "runaway" solutions exist. The eigenvalues ω corresponding to these solutions are complex.[3] The complete set of eigenfunctions $\varphi_n(z)$, including those with complex or vanishing ω, span the space of square-integrable functions on the interval $0 < z < 1$.

Figure 4.1 shows the behaviour of the first few energy levels of the φ field as a function of the strength of the external electric field, for a selection of boundary

[3] The precise condition for complex eigenvalues is either $h_0 < 0$ and $h_1 < 0$ or $h_\alpha > 0 > h_\beta$ and $-h_\beta > h_\alpha/(1 + h_\alpha)$.
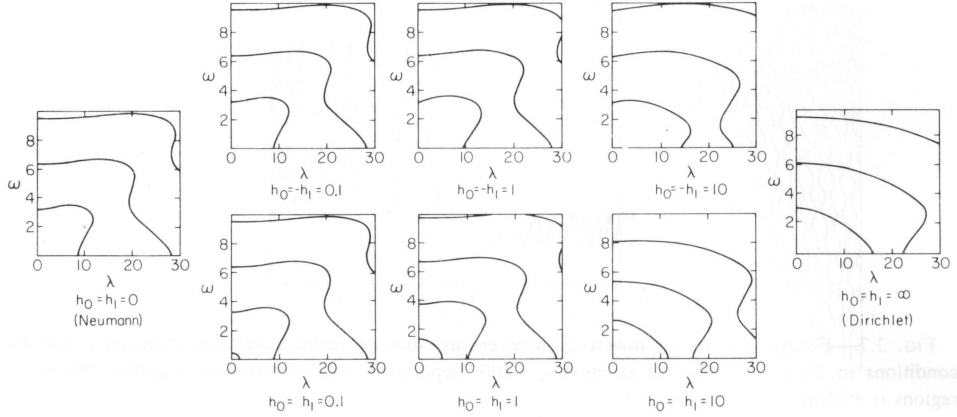
FIG. 4.1. Energy levels for a massless charged scalar field subject to a range of boundary conditions, as a function of the strength λ of an external applied electric field. h_0, h_1 parametrize general Robin boundary conditions. Dirichlet and Neumann boundary conditions are limiting cases.

conditions with $h_0 = \pm h_1$. The results interpolate smoothly between the limiting cases of Neumann boundary conditions ($h_1 = h_0 = 0$) and Dirichlet boundary conditions ($h_1 = h_0 = \infty$). When $h_1 = +h_0$. decreasing h_α shifts the energy levels as if the λ axis was shifted to move the point $\lambda = \lambda_c$ towards the origin. When $h_\alpha = 0$, the zero norm eigenfunction which appeared at $\lambda = \lambda_c$ in the Dirichlet $h_\alpha = \infty$ case appears at $\lambda = 0$, as the eigenfunction $\varphi(z) = 1$. As expected, complex modes appear immediately above $\lambda = 0$ in the Neumann $h_\alpha = 0$ case.

The presence of complex modes at small λ for Neumann boundary conditions leads to very different results for vacuum polarization than in the Dirichlet case discussed in Section 3. To first order in λ, the induced charge density associated with the nth mode satisfying Neumann boundary conditions is

$$\rho_n^I(z) = \frac{1}{2}\left[\rho_n^{(+)}(z) + \rho_n^{(-)}(z)\right] = \varepsilon\lambda\left[z(1-z) + \frac{1}{(n\pi)^2}\right]\sin(2\pi nz). \qquad (4.2)$$

This result is essentially opposite to Eq. (3.6) obtained with Dirichlet boundary conditions. The induced charge density tends to increase ("antiscreen") the electric field, rather than to decrease ("screen") it, as in the Dirichlet case.

Figure 4.2 shows the total vacuum polarization obtained by summing the contributions of all modes with real eigenvalues for $\lambda = 5$ and Neumann boundary conditions. Modes with complex eigenvalues should also appear in the sum, but no unique prescription for their inclusion exists [3, 7]. The result of Fig. 4.2 with these modes omitted clearly exhibits a positive average polarization, corresponding to an effective dielectric constant $\varepsilon < 1$. Dielectric constants in the range $0 < \varepsilon < 1$ usually imply instability [9, 10]. As discussed in Section 5, however, inclusion of back reaction effects removes complex frequency modes and yields a stable system with dielectric constant $\varepsilon > 1$.
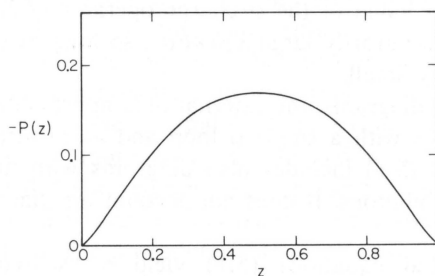
FIG. 4.2. Vacuum polarization obtained by summing modes of a massless charged scalar field subject to Neumann boundary conditions, omitting modes with complex eigenvalues. Antiscreening is evident.

Antiscreening is found at small λ whenever modes with real eigenvalues are summed, but a mode with complex eigenvalue is omitted. Boundary conditions for which no complex mode exists at sufficiently small λ always give rise to screening in this region.

5. BEYOND THE EXERNAL FIELD APPROXIMATION

Sections 3 and 4 considered the effect of a fixed classical external electric field on a charged quantized φ field. However, the φ field charge density induced by the external field itself generates an electric field, which may in turn modify the vacuum polarization. Assuming that the electric field may still be treated as classical, this "back reaction" may be included exactly. In this section, we describe the necessary procedure, and discuss results for large external electric fields including back reaction effects.

The complete result for vacuum polarization including back reaction effects is obtained by solving the coupled equations (see Section 2)

$$\left([\omega_n - \varepsilon A_0]^2 + \frac{\partial^2}{\partial z^2}\right)\varphi_n = 0, \tag{5.1a}$$

$$\rho_n = \varepsilon(\omega_n - \varepsilon A_0)|\varphi_n|^2, \tag{5.1b}$$

$$A_0 = (A_0)_0 + \frac{1}{2}\sum_{n=1}^{\infty}\int_{1/2}^{z} dz' \int_{0}^{z'} dz''(\rho_n(z'') - \rho_n(1 - z''))$$

$$= (A_0)_0 + \frac{1}{2}\int_{0}^{1} dz \left(-\frac{1}{2}|z - z'|\right)(\rho(z') - \rho(1 - z')), \tag{5.1c}$$

where $(A_0)_0$ is the original external potential. In the second form of Eq. (5.1c), the factor $-\frac{1}{2}|z - z'|$ is the Coulomb Green function in $1 + 1$ dimensions.

Equations (5.1) take a quantized φ field, but assume a classical A field depending

only on the expectation value of the φ charge operator (2.25). This approximation should be accurate for arbitrarily large $\lambda = \varepsilon E a^2$, so long as the charge ε on a single φ quantum is sufficiently small.

In terms of Feynman diagrams, the external field approximation used in Sections 3 and 4 sums all diagrams with a single φ loop and an arbitrary number of external field vertices. Equation (5.1) includes also diagrams with many φ loops in a tree connected by Coulomb photons. It does not account for diagrams involving photons within a single φ loop.

The integro-differential equations (5.1) yield a "self-consistent" solution for vacuum polarization. The equations may often be solved by a simple iterative procedure. At the first step in the procedure the vacuum polarization obtained with the original external electric field is calculated as in the external field approximation. The next step consists in calculating the correction to the electric field resulting from the vacuum polarization. This modified field is then used to calculate a new vacuum polarization. The iteration continues until a self-consistent vacuum polarization is obtained. Labelling successive steps in this procedure by the parameter κ, the necessary sequence of equations is obtained by replacing ω_n, φ_n and ρ_n by $(\omega_n)_\kappa$, $(\varphi_n)_\kappa$ and $(\rho_n)_\kappa$ respectively in Eqs. (5.1), and replacing A_0 by $(A_0)_{\kappa-1}$ in (5.1a) and (5.1b) and by $(A_0)_\kappa$ in (5.1c).

At small λ, the φ vacuum polarization obtained in the external field approximation is small. So long as ε is small, the resulting modification to the electric field is small, and back reaction effects are negligible. With Dirichlet boundary conditions at $\lambda = 10$, inclusion of back reaction effects changes the final vacuum polarization by $\sim 3\%$. As λ approaches λ_c, however, the charge density associated with the lowest mode increases, and the total vacuum polarization becomes larger. Figure 5.1 shows the total vacuum polarization at successive steps in the iterative procedure for a φ field with Dirichlet boundary conditions and $\varepsilon = 1$ close to $\lambda = \lambda_c$. $\kappa = 0$ is the
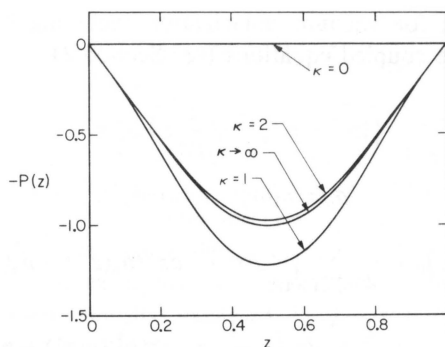

FIG. 5.1 Vacuum polarization for massless unit charge scalar field with Dirichlet boundary conditions in an external electric field with strength $\lambda = 15.5$ close to λ_c. Back reaction effects are included by an iterative procedure. The steps in the procedure are labelled by κ. $\kappa = 0$ corresponds to the original zero polarization. $\kappa = 1$ gives the external field approximation result. In the limit $\kappa \to \infty$, the vacuum polarization tends to the exact self-consistent form obtained from Eq. (5.1).

original zero vacuum polarization. $\kappa = 1$ is the result in the external field approximation. The result for $\kappa \to \infty$ is the final self-consistent one. When $\kappa > 1$, the vacuum polarization depends not only on λ, but also on the charge ε. Notice that in the case shown, the iterative procedure converges rapidly.

When λ increases above λ_c, the external field approximation yields complex energy eigenvalues, and is no longer appropriate, as discussed in Sections 3 and 4. Equations (5.1) may nevertheless still be solved iteratively if a suitable starting form for $(A_0)_1$ is chosen. Figure 5.2 shows the vacuum polarization just above $\lambda = \lambda_c$ as a function of κ for two choices of $(A_0)_1$. The procedure is seen to converge to the same final self-consistent vacuum polarization in the two cases.

When λ approaches λ_c, the energy ω_1 of the lowest mode in the external field approximation goes to zero. Figures 5.2c and 5.2d show, however, the sequence of
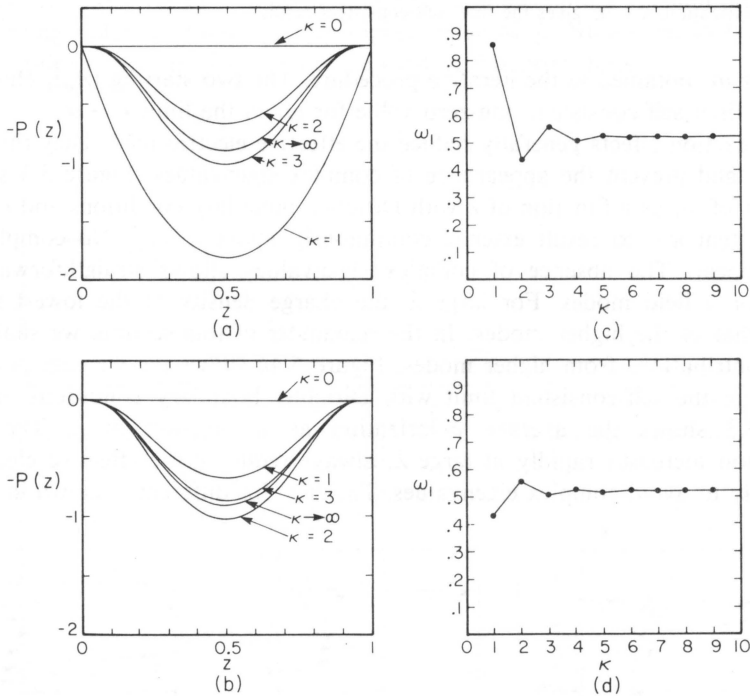

FIG. 5.2.   Results for a massless unit charge scalar field with Dirichlet boundary conditions in an external electric field just above the critical field $\lambda_c \simeq 16$. Steps in the iterative procedure used to include back reaction effects are labelled by κ. (a) and (b) show results for vacuum polarization at various stages in the iterative procedure. (c) and (d) give the behaviour of the lowest energy eigenvalue ω_1 as a function of κ. Two choices are made for the starting potential $(A_0)_1$ in the iterative procedure. (The original external electric field cannot be used because of the complex eigenvalues it yields when $\lambda > \lambda_c$.) The starting polarizations are labelled $\kappa = 1$. In (a) and (c) the potential $2\lambda_c \sinh(2(z - \frac{1}{2}))/\cosh(1)$ was used; in (b) and (d) the potential from vacuum polarization at $\lambda = 15$. The results from the two starting potentials are seen to converge to the same final $\kappa \to \infty$ self-consistent form.
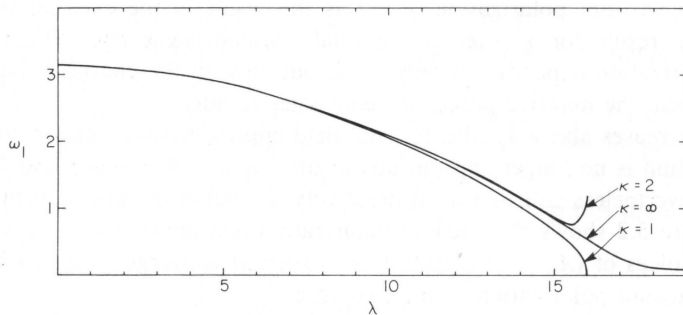
AMBJØRN AND WOLFRAM

FIG. 5.3. Behaviour of lowest positive energy level for massless unit charge scalar field with Dirichlet boundary conditions, as a function of the strength λ of an external electric field. Steps in the iterative procedure used to account for back reaction effects are labelled by κ. $\kappa = 1$ gives the external field approximation result. The curve marked $\kappa = 2$ is the second step in an iteration starting from zero vacuum polarization. $\kappa = \infty$ gives the final self-consistent result.

values for ω_1 obtained in the iterative procedure. The two starting $(A_0)_1$ chosen yield the same final self-consistent non-zero value for ω_1 in the limit $\kappa \to \infty$.

Back reaction effects generally reduce the effective electric field. They thus tend to raise ω_1, and prevent the appearance of complex eigenvalues. Figure 5.3 shows the behaviour of ω_1 as a function of λ with Dirichlet boundary conditions and $\varepsilon = 1$. The self-consistent $\kappa \to \infty$ result extends continuously above $\lambda = \lambda_c$. No complex eigenvalues appear. The absence of complex eigenvalues allows straigthforward quantization of φ field modes. For large λ, the charge density of the lowest mode far exceeds that of the higher modes. In the remainder of this section, we shall usually ignore contributions from higher modes. Figure 5.4a shows the vacuum polarization obtained in the self-consistent limit with Dirichlet boundary conditions and $\varepsilon = 1$. Figure 3.3 shows the average polarization as a function of λ. The vacuum polarization increases rapidly at large λ, always reducing the effective electric field sufficiently to avoid complex eigenvalues. The $P(z)$ for different λ shown in Fig. 5.4a
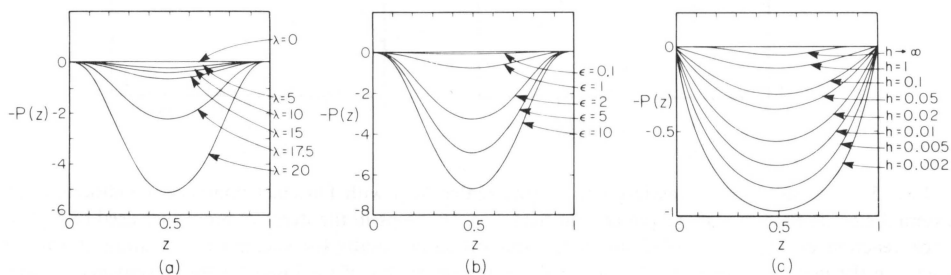

FIG. 5.4. Self-consistent results for vacuum polarization of a massless scalar field carrying charge ε induced by an external electric field of strength λ. (a) Dirichlet boundary conditions; $\varepsilon = 1$. (b) $\lambda = 15.5 \sim \lambda_c$; Dirichlet boundary conditions. (c) $\lambda = 1$; $\varepsilon = 1$; Robin boundary conditions with $h_0 = -h_1 = h$. ($h \to \infty$ corresponds to Dirichlet and $h \to 0$ to Neumann boundary conditions.) Only the lowest energy mode is included: small contributions from higher modes are dropped.

differ essentially only in overall scale. Large screening of the external electric field occurs around $z = \frac{1}{2}$, but boundary conditions on the φ field enforce zero vacuum polarization for $z = 0, 1$.

The behaviour of a physical system with a large external electric field depends on the mechanism by which the field is introduced. In typical situations, an external electric potential is increased as a function of time (for example, by separating "capacitor" plates carrying fixed electric charges). Transients resulting from a rapid increase in the electric field would mix normal modes and require a complete solution of the time-dependent Klein–Gordon equation (2.2). However, if the rate of change of the electric field is small compared to the frequency of the low modes of the field, then time-independent normal mode analysis provides an adequate approximation. As the external electric field is increased, the vacuum polarization achieves its self-consistent form at every λ. Suitable choices for $(A_0)_1$ in Eq. (5.1) are obtained by solving the equations for one value of λ, and using the resulting vacuum polarization in the starting potential for a slightly higher value of λ. Numerical instabilities in practice require rather small λ steps to be used in this procedure.
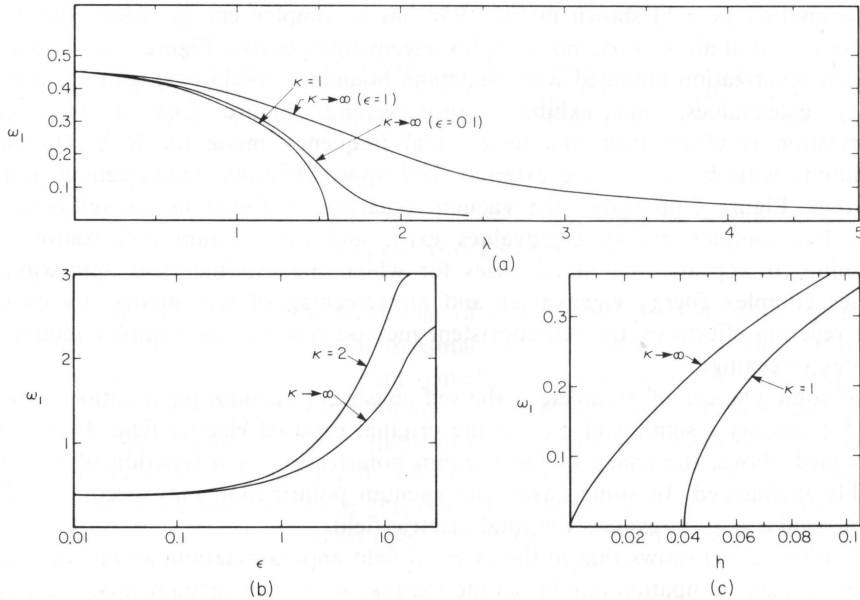

Fig. 5.5. Behaviour of the lowest positive energy level ω_1 for a massless charge ε scalar field in an external electric field of strength λ. κ labels steps in the iterative procedure used to account for back reaction effects. $\kappa = 1$ corresponds to the external field approximation. Final self-consistent results are obtained in the limit $\kappa \to \infty$. (a) ω_1 for Robin boundary conditions with $h_0 = -h_1 = 0.1$ as a function of λ. (b) ω_1 as a function of ε for Dirichlet boundary conditions with $\lambda = 15.5 \sim \lambda_c$. (c) ω_1 for $\lambda = 1$ as a function of the parameter $h = h_0 = -h_1$ specifying Robin boundary conditions. $h \to 0$ corresponds to Neumann boundary conditions.

Figure 4.1 shows that with Robin boundary conditions $h_0 = -h_1 = h$, the critical λ_c in the external field approximation decreases with decreasing h. The behaviour of ω_1 as a function of λ for $h = 0.1$ is shown in Fig. 5.5a. Once again, the self-consistent ω_1 remains non-zero above $\lambda = \lambda_c$, and no complex eigenvalues appear. Different self-consistent results are obtained for different charges ε. Smaller charge implies smaller back reaction; the value of ω_1 thus tends to be smaller for $\varepsilon = 0.1$ than for $\varepsilon = 1$, but it remains non-zero.

Figure 5.5b shows the dependence of ω_1 on ε in the presence of back reaction effects. Figure 5.4b shows the corresponding vacuum polarization. For $\varepsilon \gtrsim 10$, results become unreliable as the semiclassical approximation fails.

Figures 5.4c and 5.5c show the dependence of the vacuum polarization and first energy level on the parameter h specifying Robin boundary conditions. ω_1 remains non-zero in the self-consistent limit for all $h > 0$. As h approaches zero, corresponding to Neumann boundary conditions, however, ω_1 tends to zero. The vacuum polarization increases as ω_1 decreases. When $h = 0$, ω_1 reaches zero. As discussed in Section 4, Neumann boundary conditions lie on the edge of the Robin parameter region in which free field modes have complex eigenvalues. The Neumann case is thus at the boundary between stable and unstable systems in the self-consistent limit. For $h < h_c \simeq 0.042$, the lowest energy level in the external field approximation ($\kappa = 1$) shown in Fig. 5.5c has a complex energy eigenvalue. In the self-consistent limit $\kappa \to \infty$, no complex eigenvalues occur. Figure 4.2 showed the vacuum polarization obtained with Neumann boundary conditions, ignoring complex energy eigenvalues, and exhibited antiscreening. Figure 5.6a shows vacuum polarization resulting from the lowest real frequency mode for Robin boundary conditions with $h = 0.1$ in the external field approximation. Antiscreening is again apparent. Figure 5.6b shows the vacuum polarization found in the self-consistent limit. No complex energy eigenvalues exist, and the vacuum polarization gives screening. It appears that in all cases for which the external field approximation implies complex energy eigenvalues and antiscreening of real modes, inclusion of back reaction effects by the self-consistent method removes the complex modes, and restores screening.

For some choices of parameters, the self-consistent vacuum polarization shown in Fig. 5.4 screens a significant part of the original external electric field. However, as mentioned above, the shape of the vacuum polarization as a function of z remains roughly unchanged. In some cases, the vacuum polarization may become so large that around $z = \frac{1}{2}$, it reverses the total electric field.

Equation (2.24) shows that in the external field approximaztion, all modes of the φ field have zero occupation number in the vacuum state. The vacuum state is generally the state of lowest energy: when back reaction effects are included, the lowest energy state might involve non-zero occupation numbers (cf. [4]). Nevertheless, in the self-consistent limit it appears however that non-zero occupation numbers always increase the total energy obtained from Eq. (2.6). The vacuum state therefore remains as the unique state with zero occupation number for each mode.
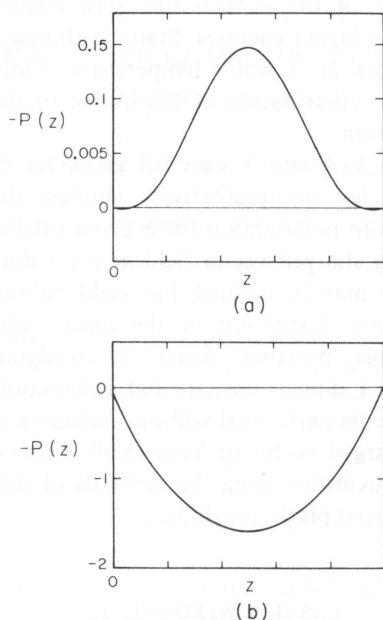
0.15

0.1

$-P(z)$

0.005

0

0   z 1

(a)

0

$-P(z)$

-1

-2

0   z 1

(b)

FIG. 5.6. Vacuum polarization associated with the lowest mode of a massless unit charge scalar field with Robin boundary conditions $h = 0.1$ in an external electric field of strength $\lambda = 2$. (a) Result in the external field approximation (ignoring complex frequency modes). (b) Result including back reaction through self-consistent procedure.

6. DISCUSSION AND EXTENSIONS

Sections 3 and 4 described the behaviour of a charged scalar field with an applied electric field in the "external field approximation." Section 5 gave results including back reaction effects by a self-consistent semiclassical procedure. Complex frequency modes indicating instabilities were found for large electric field strengths in the external field approximation. These instabilities never occurred when back reaction effects were included. The magnitude of vacuum polarization in the self-consistent limit was always found to reduce the effective electric field until no instatilities appeared. In some cases, the vacuum polarization was sufficient to reverse the electric field around $z = \frac{1}{2}$.

The self-consistent semiclassical procedure of Section 5 takes a quantized φ field and a classical electromagnetic field determined from the expectation value of φ. Results depend not only on $\lambda = eEa^2$ (as in the external field approximation), but also on the charge ε of a single φ quantum. Whereas the external field approximation fails for large λ, the semiclassical approximation is accurate for large λ, so long as $\varepsilon^2/(4\pi)$ is small. The φ field is quantized in the semiclassical approximation by decomposition into energy eigenstates in the required external electric field. In the

vacuum state, each mode of the φ field has zero occupation number: non-zero occupation numbers lead to higher energies. States with non-zero occupation numbers should, however, contribute at a finite temperature. Finite temperature typically serves only to enhance the contribution of the lowest mode, and has no qualitative effect on vacuum polarization.

The results in Sections 3, 4 and 5 were all given for massless scalar particles. Results for massive particles are qualitatively similar: the presence of the mass typically reduces the vacuum polarization for a given external electric field. There is no adequate definition of a charged vector field in $1 + 1$ dimensions with an external electric field. Spinor fields may be defined, but yield no vacuum polarization in the external field approximation. Extension of the results given here to more space dimensions is in principle possible. Scalar electrodynamics remains formally superrenormaizable in $2 + 1$ dimensions, so that calculations analogous to those of this paper may in principle be performed without including renormalization. In $2 + 1$ dimensions, non-trivial charged vector or Yang–Mills fields exist, and calculations of suitable gauge invariant quantities using the methods of this paper should explicitly exhibit antiscreening and asymptotic freedom.

REFERENCES

1. J. Ambjørn and S. Wolfram, *Ann. Phys.* **145** (1983), 1.
2. J. Ambjørn and S. Wolfram, Properties of the Vacuum: 3. Gravitational, in preparation.
3. S. A. Fulling, Varieties of Instability of a Boson Field in an External Potential and Black Hole Klein Paradoxes, King's College unpublished report (1975); Phys. Rev. D14 (1976), 1939.
4. J. Rafelski, L. P. Fulcher, and A. Klein, *Phys. Rep.* **38C** (1978), 227.
5. H. Feshbach and F. Villars, *Rev. Mod. Phys.* **30** (1958), 24.
6. H. Snyder and J. Weinberg, *Phys. Rev.* **57** (1940), 307; L. I. Schiff, H. Snyder, and J. Weinberg, *Phys. Rev.* **57** (1940), 315.
7. B. Schroer and J. A. Swieca, *Phys. Rev. D* **2** (1970), 2938.
8. W. Magnus, F. Oberhettinger, and R. P. Soni, "Formulas and Theorems for the Special Functions of Mathematical Physics," 3rd ed., Springer-Verlag, Berlin/Heidelberg/New York, 1966.
9. O. V. Dolgov, D. A. Kirzhnits, and E. G. Maksimov, *Rev. Mod. Phys.* **53** (1981), 81.
10. L. D. Landau and E. M. Lifshitz, "Electrodynamics of Continuous Media," Sect. 14, Pergamon, 1960.
11. C. Cole, S. Wolfram, *et al.*, "SMP Handbook," Caltech, 1981.